

Improvement of Infrared Imaging Video Bolometer Systems in LHD^{*)}

Kiyofumi MUKAI, Byron J. PETERSON, Shwetang N. PANDYA¹⁾, Ryuichi SANO¹⁾
and Muneji ITOMI²⁾

National Institute for Fusion Science, Toki 509-5292, Japan

¹⁾*The Graduate University for Advanced Studies, Toki 509-5292, Japan*

²⁾*Graduate School of Engineering Hokkaido University, Sapporo 060-8628, Japan*

(Received 10 December 2013 / Accepted 19 February 2014)

The InfraRed imaging Video Bolometer (IRVB) is a powerful diagnostic to measure a plasma radiation profile especially for three-dimensional measurements. An IRVB mainly consists of a pinhole camera section and an IR camera section. The plasma radiation profile is projected on a thin metal foil through an aperture in the pinhole camera resulting in a two-dimensional temperature distribution. Then, the distribution is observed from the back side by an IR camera as an IR image. Since the image contains the effects of heat diffusion, a calibration of the heat characteristics of the foil is needed to obtain the radiation profile by solving the two-dimensional heat diffusion equation. Some deposition was observed on the foil in the Large Helical Device (LHD) plasma experiment. The effect of this on the heat characteristics of the foil should be studied although it can be compensated for by the calibration. Currently four IRVBs are operating in LHD to investigate the radiation collapse and plasma detachment phenomena. The sensitivities of IRVBs at the 6.5-L and 10-O ports were improved from the experimental campaign in FY 2013 by replacing the IR cameras of these ports. The sensitivity at the 6.5-U port was also improved by applying the periscope system.

© 2014 The Japan Society of Plasma Science and Nuclear Fusion Research

Keywords: bolometer, imaging, IRVB, radiation measurement, LHD, radiation collapse, plasma detachment

DOI: 10.1585/pfr.9.3402037

1. Introduction

Radiation profile measurements are a key to investigating plasma detachment and radiation collapse phenomena. It is known that the radiation from the ergodic region plays an important role in the phenomena [1, 2]. Therefore, the three-dimensional measurement of radiation profiles is required to study them in more detail since the radiation from the ergodic region has a three-dimensional structure. The InfraRed (IR) imaging Video Bolometer (IRVB) [3] is a useful diagnostic to investigate the plasma radiation profile. It has a large number of channels and this characteristic is an advantage for a tomography technique to reconstruct the three-dimensional radiation profile.

Currently, four IRVB systems are operating in LHD. In this study, the sensitivities of three IRVBs were improved by replacing the IR cameras or applying the periscope system. The remainder of this paper is organized as follows. In Sec. 2, the schematic of the IRVB is described. In Sec. 3, the calibration of the foil heat characteristics and the effect of the plasma discharge on the foil are expressed. In Sec. 4, IRVB systems in LHD and the improvement of their sensitivities are described before the summary in Sec. 5.

author's e-mail: mukai.kiyofumi@LHD.nifs.ac.jp

^{*)} This article is based on the presentation at the 23rd International Toki Conference (ITC23).

2. Infrared Imaging Video Bolometer

The schematic of an IRVB is shown in Fig. 1. An IRVB mainly consists of a pinhole camera section and an IR camera section. The plasma radiation profile is projected through an aperture in the pinhole camera part onto a thin metal foil held in a copper frame resulting in a two-dimensional temperature distribution. Both sides of the foil are blackened by carbon to increase the emissivity. The distribution is observed from the back side by an IR camera as an IR image through some optics and a vacuum window. They are made with ZnSe, CaF₂ or Ge and the choice of material depends on the waveband of the IR camera. The IR camera is stored in a magnetic shield, which is made with soft iron, and controlled remotely by a computer through Ethernet cables and optical fibers.

3. Calibration of Foil Heat Characteristics

3.1 Two-dimensional heat diffusion equation

The IR image which is observed by the IR camera contains the effects of heat diffusion. Therefore, the two-dimensional heat diffusion equation shown in Equation (1) should be solved to obtain the plasma radiation P_{rad} .

$$-\Omega_{\text{rad}} + \Omega_{\text{bb}} + \frac{1}{\kappa} \frac{\partial T}{\partial t} = \frac{\partial^2 T}{\partial x^2} + \frac{\partial^2 T}{\partial y^2}, \quad (1)$$

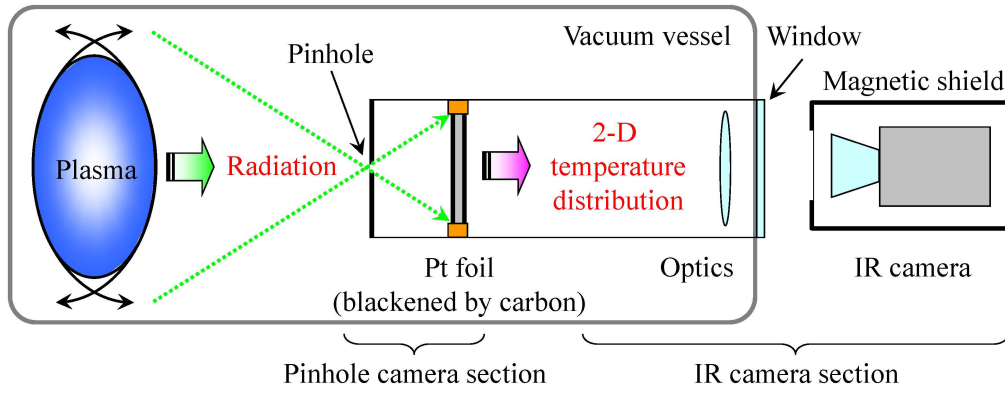


Fig. 1 Schematic of IRVB.

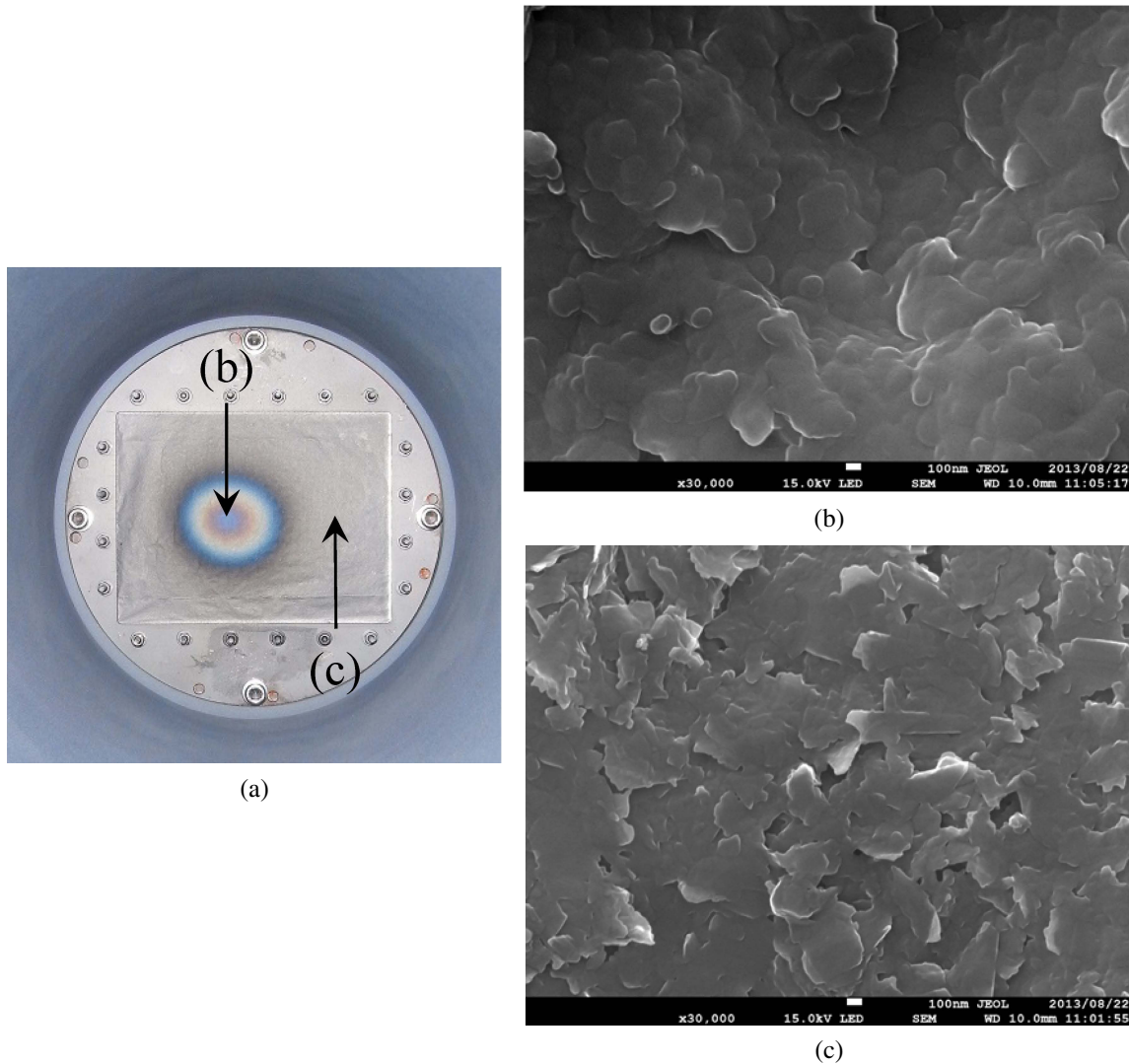


Fig. 2 Images of IRVB foil applied to LHD plasma experiment. (a) IRVB foil applied to LHD plasma experiment. (b) is deposited part and (c) is non-deposited part. (b) SEM image of carbon coating layer on Pt foil at deposited part ($\times 30,000$). (c) SEM image of carbon coating layer on Pt foil at non-deposited part ($\times 30,000$).

where Ω_{rad} is the term of the absorbed plasma radiation

$$\Omega_{\text{rad}} = \frac{P_{\text{rad}}}{kt_f l^2}, \tag{2}$$

and Ω_{bb} is the term of the IR radiation to the IR camera

$$\Omega_{\text{bb}} = \frac{\epsilon \sigma_{\text{S-B}} (T^4 - T_0^4)}{kt_f}. \tag{3}$$

Here, κ is thermal diffusivity, k is thermal conductivity, t_f is foil thickness, l^2 is foil pixel area, ϵ is emissivity, $\sigma_{\text{S-B}}$

is the Stefan-Boltzmann coefficient and T_0 is background temperature. The profile of κ , k , t_f and ε on the foil should be estimated to determine P_{rad} from Equation (1). Currently, these parameters except κ are calibrated using the comparison between a laser irradiation experiment and a finite element method (FEM) [4]. κ is assumed to be a typical value in the current method.

3.2 Effect of plasma discharge on foil

Figure 2 (a) shows the IRVB foil applied to the LHD plasma experiment. The obviously discolored area (b) was observed. Scanning electron microscope (SEM) images of the surface of the carbon coating layer are shown in Figs. 2 (b) and (c) at the discolored area and non-discolored area, respectively. Some deposition is observed at the discolored area while the non-discolored area has a flaky structure of the carbon coating. The effect of this on the heat characteristics of the foil should be studied although it can be compensated for by the calibration.

4. Improvement of IRVB Systems in LHD

4.1 Field of views of IRVBs

Four IRVB systems are operating in LHD. The FoVs

in the LHD equatorial plane are shown in Fig. 3. Figure 4 (a)-(d) show the FoVs of each IRVB. IRVBs at 6-T and 10-O ports have a tangential view in the clockwise di-

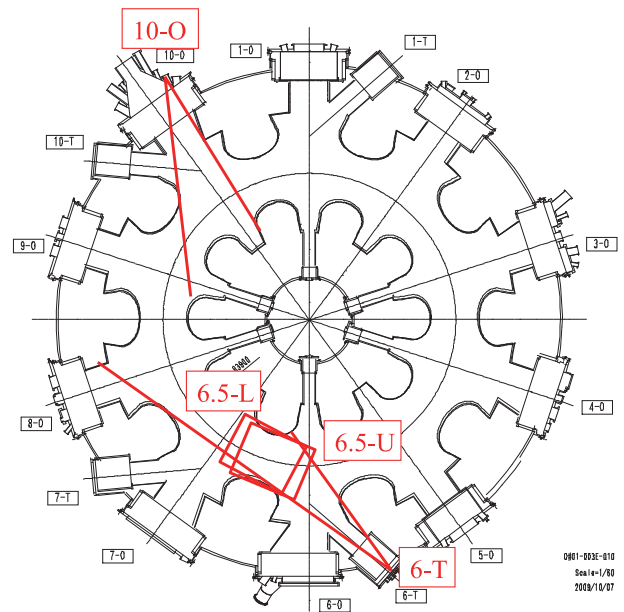
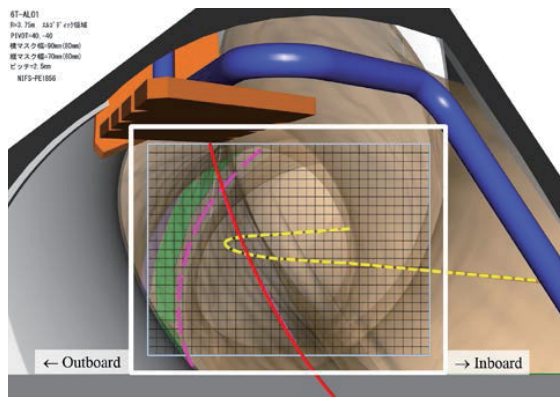
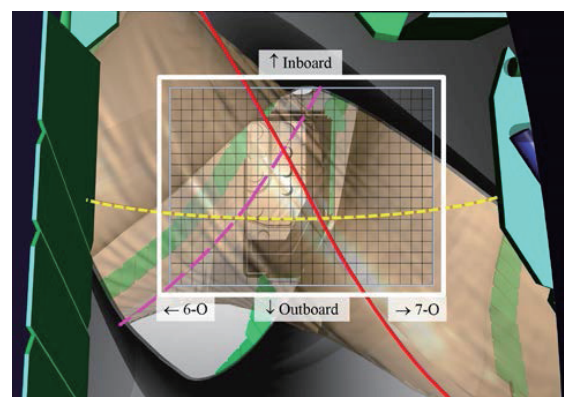


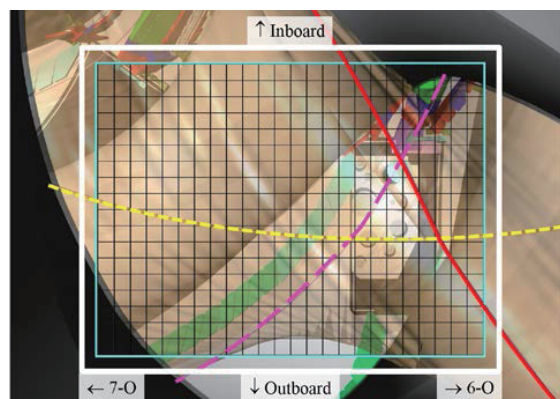
Fig. 3 Location of IRVBs in LHD.



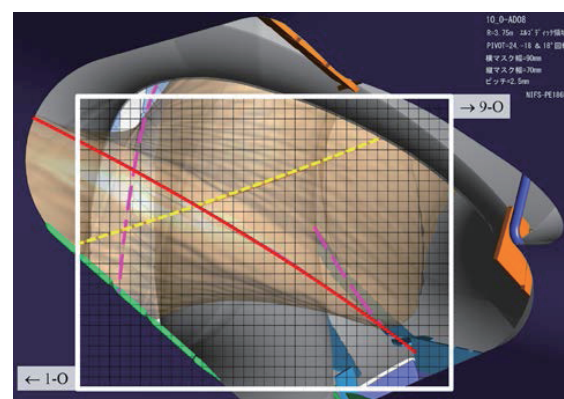
(a) 6-T port (tangential view).



(c) 6.5-L port (vertical view from bottom).



(b) 6.5-U port (vertical view from top).



(d) 10-O (semi-tangential view).

Fig. 4 FoVs of four IRVBs in LHD (white rectangular). Solid (red) and dashed (pink) lines indicate upper and lower helical divertor X-points, respectively. Short dashed line (yellow) shows magnetic axis.

Table 1 Specifications of IRVB systems in LHD.

| Port | 6-T | 6.5-U | 6.5-L | 10-O |
|-------------------------------------|-------------|-------------|-------------|-------------|
| Pinhole size [mm×mm] | 4×4 | 8×8 | 8×8 | 4×4 |
| Foil size [cm×cm] | 9×7 | 13×10 | 15×11 | 9×7 |
| Foil thickness t_f [μm] | 2.5 | 2.5 | 2.5 | 2.5 |
| Camera | FLIR/SC4000 | FLIR/A655sc | FLIR/A655sc | FLIR/SC7600 |
| λ [μm] | 3-5 | 7.5-13 | 7.5-13 | 3-5 |
| Camera pixels | 320×256 | 640×480 | 640×480 | 640×512 |
| Operating frame rate f_{IR} [fps] | 100 | 50 | 100 | 100 |
| NETD [mK] | <25 | <50 | <50 | <25 |

Table 2 Improvement of IRVB parameters in LHD.

| Port | 6-T | 6.5-U | 6.5-L | 10-O |
|----------------------------------|---------|-------------------|-----------------|-------------------|
| NETD [mK] | 25 | 50 | 100 → 50 | 100 → 25 |
| F number | 1.35 | 1 → 1.35 | 2 → 1 | 1 → 1.15 |
| N_{bol} | 18×14 | 26×20 | 30×22 | 18×14 |
| N_{IR} | 307×237 | 180×149 → 528×408 | 80×63 → 171×126 | 227×171 → 586×458 |
| A_f [cm ²] | 9×7 | 13×10 | 15×11 | 9×7 |
| f_{bol} [fps] | 100 | 100 → 50 | 30 → 100 | 60 → 100 |
| f_{IR} [fps] | 100 | 100 → 50 | 30 → 100 | 60 → 100 |
| S_{IRVB} [μW/cm ²] | 395 | 687 → 226 | 4400 → 884 | 988 → 206 |

rection and a semi-tangential view in the counter clockwise direction, respectively, and the other IRVBs at 6.5-U and 6.5-L ports have vertical views for the three-dimensional tomography. These four FoVs can cover the whole region of the LHD plasma with the assumption of a helical periodicity [5].

4.2 IRVB systems in LHD

The specifications of the four IRVBs are shown in Table 1. Here, NETD means noise equivalent temperature difference of the IR camera. Pt has been utilized for the material of all foils. CaF₂ and ZnSe vacuum windows are used for the IR cameras of shorter and longer wavelengths, respectively. RAM disks are applied as data storage for fast data acquisition.

These systems were improved from the experimental campaign in FY 2013: by (i) replacement of the IR cameras at the 6.5-L and 10-O ports, (ii) installation of a periscope system at the 6.5-U port. The IR cameras at the 6.5-L and 10-O ports were replaced from FLIR/Omega to FLIR/A655sc and FLIR/SC500 to FLIR/SC7600, respectively. The periscope system has been installed at the 6.5-U port to fit the field of view of the IR camera to the foil [6]. It consists of 3 camera lenses, a mirror and 3 relay lenses (including 2 in-vessel lenses). These lenses are made of ZnSe and Ge.

4.3 Sensitivities of the IRVBs

The sensitivities of the IRVBs at the 6.5-U, 6.5-L and 10-O ports were improved by the above upgrades. The sensitivity of the IRVB can be expressed as a noise equivalent

power difference (NEPD) S_{IRVB} in Equation (4) [7].

$$S_{IRVB} = \frac{\sqrt{2}kt_f\sigma_{IR}}{\sqrt{f_{IR}N_{IR}}} \sqrt{\frac{5N_{bol}^3f_{bol}}{A_f^2} + \frac{N_{bol}f_{bol}^3}{k^2}}. \quad (4)$$

Here, k is the thermal diffusivity and 0.716 W/(cm·K) is used as the typical value of platinum. t_f is the foil thickness and 2.5 μm is assumed. σ_{IR} is the NETD of the IR camera including the effect of the F number of the optics and the maximum value of the specification of each camera divided by the square of the F number is applied. N_{bol} is the number of IRVB pixels and one IRVB pixel corresponds to 5 × 5 mm² on the foil. N_{IR} is the number of IR camera pixels utilized in the evaluation of the IR image in the LHD plasma experiment. A_f is the utilized area of the foil which corresponds to the foil size. f_{bol} is the frame rate of IRVB which is assumed to be the operating frame rate of the IR camera f_{IR} .

The improvement of the IRVB parameters at the three ports are shown in Table 2. N_{IR} at the 6.5-U port increased by applying the periscope system. Then, the S_{IRVB} at the 6.5-U port improved from 687 μW/cm² to 226 μW/cm². N_{IR} at 6.5-L and 10-O ports increased by replacing the IR cameras. Moreover, the NETD at 6.5-L and 10-O ports are decreased respectively from 85 mK to 50 mK and from 70 mK to 25 mK. Then, the S_{IRVB} at the 6.5-L and 10-O ports improved from 4400 μW/cm² to 884 μW/cm² and from 988 μW/cm² to 206 μW/cm², respectively. The S_{IRVB} at the 6-T port is 395 μW/cm² although there is no improvement this time.

5. Conclusions

Four IRVBs are operating for the plasma radiation measurement in LHD. The sensitivities of two IRVBs (NEPD) at the 6.5-L and 10-O ports were improved from the experimental campaign in FY 2013 by replacing the IR cameras. The NEPD at the 6.5-U port was also improved by fitting the field of view of the IR camera to the foil using the periscope system. Some deposition was observed on the foil. The effect of this on the heat characteristics of the foil which correspond to the conversion coefficients from the IR images to the radiation profile should be studied to investigate in detail the radiation collapse and plasma de-

tachment phenomena and to reconstruct the 3D radiation profile of the LHD plasma.

- [1] M. Kobayashi *et al.*, Phys. Plasmas **17**, 056111 (2010).
- [2] B.J. Peterson *et al.*, J. Nucl. Mater. **415**, S1147 (2011).
- [3] B.J. Peterson *et al.*, Rev. Sci. Instrum. **70**, 3696 (2000).
- [4] R. Sano *et al.*, Plasma Fusion Res. **7**, 2405039 (2012).
- [5] R. Sano *et al.*, Plasma Fusion Res. **8**, 2402138 (2013).
- [6] S.N. Pandya *et al.*, 40th EPS Conference on Plasma Physics (2012) P5.107.
- [7] B.J. Peterson *et al.*, Rev. Sci. Instrum. **79**, 10E301 (2008).